

Finite-temperature $Sp(4)$ Yang-Mills theory: towards the continuum

Fabian Zierler ^{a,b,c,*} Ed Bennett ^{b,d} Biagio Lucini ^{e,d,f} David Mason ^g
Maurizio Piai ^{b,c} Enrico Rinaldi ^{e,h} and Davide Vadicchino ⁱ

^aTechnical University of Munich, TUM School of Natural Sciences, Physics Department, James-Franck-Str. 1, 85748 Garching bei München, Germany

^bCentre for Quantum Fields and Gravity, Faculty of Science and Engineering, Swansea University, Singleton Park, SA2 8PP, Swansea, United Kingdom

^cDepartment of Physics, Faculty of Science and Engineering, Swansea University (Park Campus), Singleton Park, SA2 8PP Swansea, Wales, United Kingdom

^dSwansea Academy of Advanced Computing, Swansea University (Bay Campus), Fabian Way, SA1 8EN Swansea, Wales, United Kingdom

^eSchool of Mathematical Sciences, Queen Mary University of London, Mile End Road, London, E1 4NS, United Kingdom

^fDepartment of Mathematics, Faculty of Science and Engineering, Swansea University (Bay Campus), Fabian Way, SA1 8EN Swansea, Wales, United Kingdom

^gJülich Supercomputing Centre, Forschungszentrum Jülich, D-52425 Jülich, Germany

^hRIKEN Center for Quantum Computing, RIKEN, 2-1 Hirosawa, Wako, Saitama, 351-0198, Japan

ⁱCentre for Mathematical Science, University of Plymouth, Plymouth, PL4 8AA, United Kingdom

E-mail: fabian.zierler@tum.de



(on behalf of the TELOS collaboration)

We present numerical results obtained in a finite-temperature study of the $Sp(4)$ Yang-Mills theory on the lattice. We study its first-order confinement/deconfinement phase transition, by reconstructing the density of states via the Logarithmic Linear Relaxation (LLR) algorithm. We perform our measurements on lattices with different extents of space and time (and aspect ratios). We estimate the size of discretisation and finite-volume artefacts. We find clear signatures of a first-order transition. We determine the critical coupling, the specific heat, and the surface tension, for finite extents of the thermal circle, and use the results to set bounds for the continuum theory.

The 42nd International Symposium on Lattice Field Theory (LATTICE2025)

2-8 November 2025

Tata Institute of Fundamental Research, Mumbai, India

*Speaker

1. Introduction

Non-Abelian, confining gauge theories, possibly coupled to new fermion matter field content, are promising candidates for the short-distance completion of proposals for Beyond the Standard Model (BSM) physics with composite dynamical origin. Their properties can be used to address a broad range of open phenomenological questions, ranging from the origin of dark matter, to electroweak and Higgs physics, and to the generation of mass of SM fermions—see for instance the reviews in Refs. [1–4] and references therein. One of the exciting aspects of some of these theories is that they lead to a relic stochastic background of gravitational waves (GWs), if the new physics underwent a phase transition in the early universe [5]. This signal is potentially detectable by the next generation of ground and space based experiments [6, 7]. Yet, computing a precise prediction of the gravitational wave power spectrum is not straightforward. To determine the gravitational wave spectrum within the thin-wall approximation, one requires knowledge of the latent heat and the confined-deconfined surface tension [8–10], which are the subjects of the $SU(N)$ lattice studies in Refs. [11–13]. Alternative approaches based on models involving the Polyakov loop have also been proposed—see for instance Refs. [8, 14, 15].

The strongly coupled nature of non-Abelian gauge theories requires non-perturbative tools in order to make theoretical predictions. The methods of lattice field theory provide a first-principles, systematically improvable approach to determine numerically the non-perturbative properties of these theories. They rely on sampling the space of possible gauge field configurations, $\{U\}$, to determine the expectation value, or ensemble average, of operators of interest, O , defined as

$$\langle O \rangle = \frac{1}{Z} \int D[U] O[U] \exp(-\beta S[U]) , \quad (1)$$

where the normalisation of the ensemble average is given by

$$Z = \int D[U] \exp(-\beta S[U]) . \quad (2)$$

The existence of first-order phase transitions in Yang-Mills theories has been established numerically for gauge theories with $SU(N > 2)$ [11, 13, 16, 17], $Sp(2N > 2)$ [18], and G_2 [19, 20] gauge group. It is challenging to achieve the required precision with standard lattice algorithms based on importance sampling, as their effectiveness is limited in the presence of a first-order phase transition. Due to the phenomenon of phase coexistence, the distribution in Eqs. (1) and (2) has a bimodal character in the proximity of the transition, and standard importance sampling algorithms struggle to sample the path integral efficiently, because the Markov chains tend to get stuck in one phase.

The Logarithmic Linear Relaxation (LLR) algorithm [21, 22] provides an alternative algorithm to describe Yang-Mills theories in proximity of a first-order phase transition. Building on our earlier work on $SU(3)$ on a fixed lattice volume [23], and on the thermodynamic limit $Sp(4)$ for fixed thermal circle, $N_t = 4$ [24], in this contribution we present new results for $Sp(4)$ with $N_t = 5$. This research is a necessary step towards the continuum limit. More details can be found in Ref. [25].

2. Density-of-states & Logarithmic Linear Relaxation

We circumvent the limitations of importance sampling methods by using an approach based on the density of states, $\rho(E)$. For operators that depend only on the energy, $O(S[U] = E)$, we rewrite

Eqs. (1) and (2) as a one dimensional integral over the energy

$$\langle O \rangle = \frac{1}{Z} \int dE \rho(E) O(E) \exp(-\beta S[E]) , \quad (3)$$

$$Z = \int dE \rho(E) \exp(-\beta S[U]) , \quad (4)$$

where we have defined the density of states as

$$\rho(E) = \int D[U] \delta(S[U] - E) . \quad (5)$$

In order to determine the density of states precisely and reliably, we follow the process outlined in Ref. [21, 22], and employ a linear logarithmic approximation of the density of states. We write

$$\rho(E) = \rho(0) \exp \left[- \int_0^E d\bar{E} a(\bar{E}) \right] , \quad (6)$$

where $a(E)$ is a piecewise-linear function, defined by splitting the energy into small intervals. The coefficients a_n and c_n determine the density of states as

$$\log \rho(E) \simeq a_n (E_n^0 - E) + c_n , \quad (7)$$

in a given interval centred around E_n^0 . The coefficients c_n are determined from requiring continuity—up to the first coefficient, c_0 , which corresponds to $\rho(0)$ and drops out of the ensemble averages.

The remaining coefficients, a_n , are determined by considering the following expectation value, which we denote with double brackets:

$$\langle\langle O \rangle\rangle(\hat{a}) = \int D[A] O[A] W(E_n, \delta) \exp[(S[A] - E_n) \hat{a}] , \quad (8)$$

and where we introduced the function

$$W(x, \delta) = \begin{cases} 1 & \text{if } x \in [-\delta/2, +\delta/2] \\ 0 & \text{else} \end{cases} , \quad (9)$$

in which \hat{a} is for now an arbitrary parameter. The purpose of W is to restrict the energy range to a finite interval. We compute a_n by setting $O = S[A] - E_n$ and requiring its vanishing

$$\langle\langle O = S[A] - E_n \rangle\rangle(\hat{a} = a_n) = 0 . \quad (10)$$

To find the (unique) root of Eq. (10), and hence a_n , we define a stochastic, non-linear, iterative process, with the following prescription for the $(i + 1)$ -th iteration step

$$a_n^{(i+1)} = a_n^{(i)} - b^{(i)} \langle\langle S[A] - E_n \rangle\rangle(a_n^{(i)}) . \quad (11)$$

Initially, we start with several Newton-Raphson update steps, for which $b_i \equiv 1$. Then we adopt the simple choice $b_i = 1/i$ for the Robbins-Monro prescription, that satisfy the relations

$$\sum_i b_i \rightarrow \infty , \quad \sum_i b_i^2 = \text{finite} . \quad (12)$$

Table 1: Lattice parameters controlling the LLR algorithm for the $Sp(4)$ Yang-Mills theory.

N_t	N_s	u_p^{\min}	u_p^{\max}	N_{rep}	N_{repeats}	n_{NR}	n_{RM}
5	48	0.588	0.592	48	25	10	60
5	48	0.588	0.592	96	25	10	50
5	56	0.588	0.592	128	25	10	50
5	56	0.588	0.592	48	25	10	50
5	56	0.588	0.592	96	25	10	50
5	64	0.588	0.592	95	20	7	50
5	72	0.588	0.592	95	20	11	50
5	80	0.588	0.59	64	20	15	30

This procedure may be affected by a potential ergodicity problem. By constraining every Markov chain to a single energy interval when calculating $\langle\langle O \rangle\rangle$, we might miss gauge configurations with energies in the same interval that are only connected via intermediate energies outside the selected interval. To circumvent this potential issue, we implement additionally a *parallel tempering* approach. We consider energies in the range $[E_{\min}, E_{\max}]$ and choose N_{rep} evenly-spaced, overlapping intervals and start a Markov chain for every energy interval. After every update we swap the Markov chains of two neighbouring intervals, n and $n + 1$, with a probability of

$$P_{\text{swap}} = \min \left(1, e^{(S[A^{(n)}] - S[A^{(n+1)}])(a^{(n)} - a^{(n+1)})} \right). \quad (13)$$

We allow the first and last interval to probe energies below E_{\min} and above E_{\max} , respectively.

3. Lattice Setup

We express the Wilson gauge action in terms of the plaquette, $U = U_{\mu\nu}$, as

$$S[U] = \frac{1}{N_c} \sum_x \sum_{\mu < \nu} \text{Re Tr} [1 - U_{\mu\nu}(x)] \equiv 6N_t N_s^3 (1 - u_p[U]), \quad (14)$$

where $N_c = 2N = 4$ for $Sp(4)$. The hypercubic lattice has lattice spacing a and N_t lattice sites in the temporal (thermal) direction and N_s lattice sites in the space directions. The averaged plaquette, u_p , will be later used as a proxy for the energy, E . We impose periodic boundary conditions, and interpret the temporal lattice extent (with $N_t < N_s$) in terms of the equilibrium temperature. We use the HiRep code [26, 27] extended to symplectic gauge groups [28] with support for the LLR based on restricted heatbath updates with domain decomposition and over-relaxation [23, 29].

We show the value of the lattice parameters used for the LLR study in table 1. The energy range corresponds to values of the average plaquette in the interval $[u_p^{\min}, u_p^{\max}]$, divided in N_{rep} small intervals. We use n_{NR} Newton-Raphson updates followed by n_{RM} Robbins-Monro updates. In evaluating the double bracket expectation value in Eq. (8), we first perform 300 thermalisation steps, followed by 700 measurement steps. We estimate the overall uncertainties by repeating the iteration procedure N_{repeat} times and performing a jackknife resampling analysis among all repetitions.

4. Observables

We first consider the probability distribution for a given energy, E , defined as

$$P_\beta(E) = \frac{1}{Z(\beta)} \rho(E) e^{-\beta E}. \quad (15)$$

At the critical coupling, β_c , the two phases coexist and the distribution must show two peaks. At finite spatial volume, we can define the critical coupling by dialling it until the peaks have equal heights. The density of states does not depend on β , and, once we have obtained $\rho(E)$, this tuning can determine β_c very accurately.

We can further use the probability density to estimate the interface tension from the height of the peaks of the distribution relative to the height of an intermediate plateau arising in the interval between them, due to the presence of an interface. We estimate this effect by considering the minimal value of P_β between the two maxima, which in the thermodynamic limit takes the form

$$\frac{P_{\min}}{P_{\max}} \propto \sqrt{N_s} \exp\left(-2 \frac{N_s^2}{N_t^2} \frac{\sigma_{cd}}{T_c^3}\right). \quad (16)$$

We measure the quantity

$$\tilde{I} \equiv -\frac{1}{2} \left(\frac{N_t}{N_s}\right)^2 \log\left(\frac{P_{\min}}{P_{\max}}\right) + \frac{1}{4} \left(\frac{N_t}{N_s}\right)^2 \log(N_s), \quad (17)$$

which in the thermodynamic limit satisfies $\lim_{N_s/N_t \rightarrow \infty} \tilde{I} = \frac{\sigma_{cd}}{T_c^3}$.

Alternative definitions of β_c are provided by the maximum of the specific heat, $C_V(\beta)$, and the minimum of the Binder cumulant, $B_V(\beta)$, respectively:

$$C_V(\beta) \equiv \frac{6V}{a^4} \left[\langle u_p^2 \rangle_\beta - \langle u_p \rangle_\beta^2 \right], \quad B_V(\beta) \equiv 1 - \frac{\langle u_p^4 \rangle_\beta}{3 \langle u_p^2 \rangle_\beta^2}. \quad (18)$$

While these determinations of β_c are guaranteed to coincide in the thermodynamic limit, this is not the case at finite volume.

5. Results

On the left-hand-side in Fig. 1, we show the final values of a_n plotted against the central value of the average plaquette, u_p . We observe excellent agreement between results obtained with the same lattice parameters, when varying the number of energy intervals. From this, we conclude that the chosen interval widths are sufficiently small as to not induce sizeable systematic artefacts.

On the right panel of Fig. 1, we compare the final values obtained for a_n , for different choices of lattice volume. Starting at an aspect ratio of $N_s/N_t = 9.6$ we start to observe a_n being multi-valued in u_p , indicating the presence of a first order-transition. This behaviour becomes more pronounced as the spatial volume (and aspect ratio) is increased. We observe that the required aspect ratios are larger than the values that were sufficient for $N_t = 4$ [24]. Consequently, the computational cost for finer lattices grows substantially.

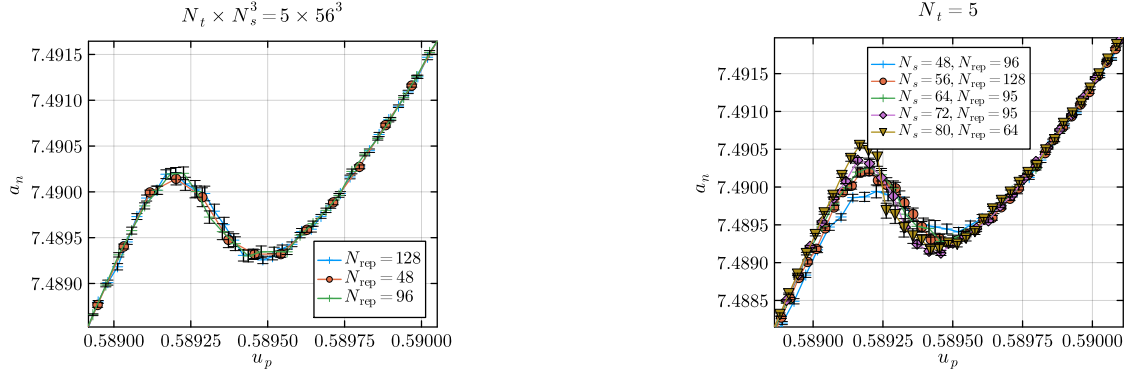


Figure 1: Left panel: final result for a_n as a function of the average plaquette, u_p , evaluated at the centre of the intervals, for fixed choice of lattice volume, and by varying the number of energy intervals. Right panel: final results for a_n as a function of the average plaquette, u_p , evaluated at the centre of the intervals, for all spatial volumes considered, with fixed $N_t = 5$.

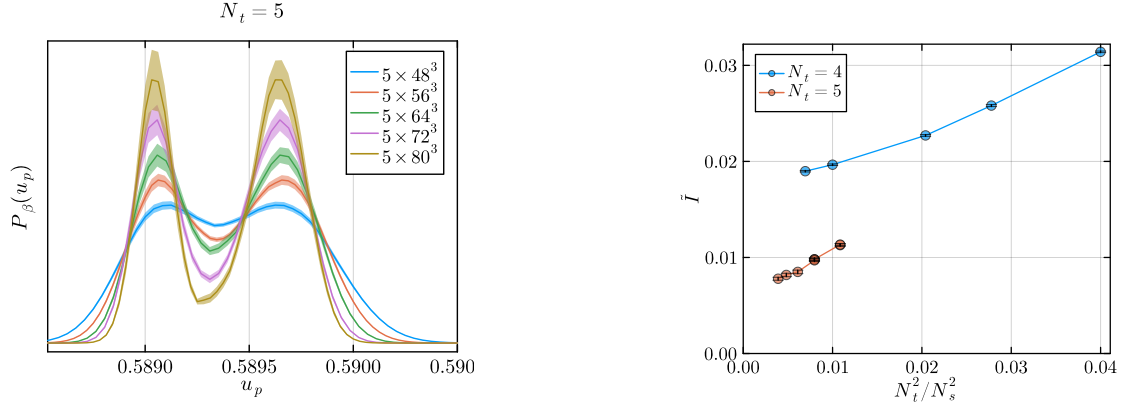


Figure 2: Left panel: probability distribution, $P_\beta(u_p)$, against the central value of the average plaquette. The inverse gauge coupling, β , has been tuned such that the maxima are of equal height. Right panel: surface tension term, \tilde{I} , extracted at finite volume, according to Eq. (17).

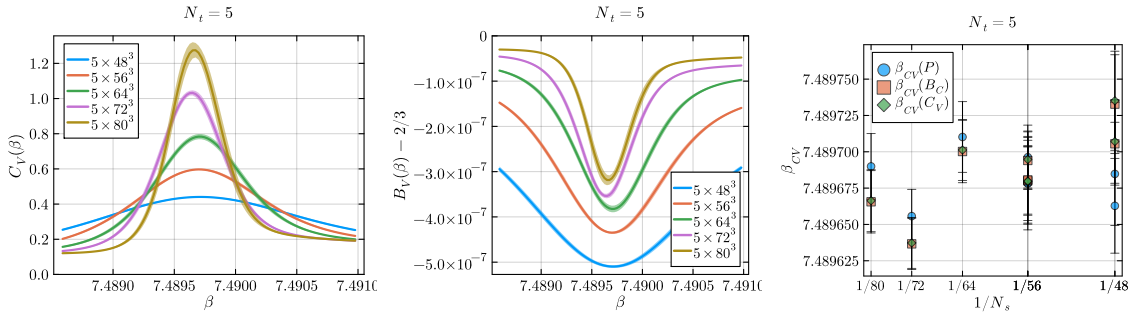


Figure 3: Left panel: specific heat, C_V , as a function of β . Middle panel: Binder cumulant, B_V , as a function of β . In both case, the position of the extrema yields a determination of the critical coupling. Right panel: comparison between inverse critical coupling, β_c , as determined from the plaquette distribution (P), the specific heat (C_V), and the Binder cumulant (B_V).

In Fig. 2, in the left panel, we show the plaquette probability distribution tuned to the critical coupling for all available spatial volumes. A separation develops between the two peaks as the volume increases. Unfortunately, as in the case of $N_t = 4$ [23], we do not observe the formation of a clear plateau in the interstice between peaks. In the right panel of the same figure, we show an estimate of the interface tension, \tilde{I} , defined in Eq. (17), for both $N_t = 4$ (based on the previously published numerical results) and $N_t = 5$. We observe that \tilde{I} for $N_t = 5$ is approximately half of the results obtained at $N_t = 4$. This finding is indicative of the presence of discretisation artefacts. This result should be assessed with the caveat that our analysis uses the local minimum of the probability distribution a proxy for the eventual plateau. In the future, it might be helpful to address this point to consider the approach used in Ref. [13] and elongate one of the spatial dimensions to provide a preferred direction for the formation of an interface.

In Fig. 3, we show both the specific heat (left panel) and the Binder cumulant (middle), defined in Eqs. (18). We observe the clear formation of local extrema, allowing a determination of the critical coupling. When comparing the resulting estimates of β_c with the ones obtained from the plaquette distribution, we find agreement (within errors) for all volumes (right panel). Additionally, we observe only a moderate volume dependence. This conclusion is in stark contrast with Ref. [23], that reported sizeable volume dependence as well as a tension between different methodologies. This is interpreted as an encouraging partial result, in the approach to the continuum.

We close this report by commenting on early trends emerging from our analysis of ensembles with $N_t = 6$, which form the starting point of a future project. We have been so far unable to identify an energy range exhibiting clear visible signal of a first-order transition, for lattice volumes up to 6×72^3 , corresponding to aspect ratios larger than the ones needed for $N_t = 4, 5$. This finding is in line with the trend observed in transitioning between $N_t = 4$ and $N_t = 5$.

6. Summary

We have determined several observable quantities associated with the thermal first-order transition characterising deconfinement for the $Sp(4)$ Yang-Mills theory. We considered ensembles with $N_t = 5$, which extend and complement previous calculations performed with $N_t = 4$. This serves as a step towards the continuum extrapolation. We demonstrated that finite volume effects are controllable, and that the systematics related to the methodology are reduced, in respect to $N_t = 4$. Overall, the picture of a comparatively weak, first-order phase transition emerges.

Acknowledgments

We thank Stephan J. Huber, David Mateos, and Manuel Reichert for useful discussions, and Frederic D. R. Bonnet for help in benchmarking our code.

E.B. and B.L. were supported by the EPSRC ExCALIBUR programme ExaTEPP (project EP/X017168/1). E.B. was supported by the STFC Research Software Engineering Fellowship EP/V052489/1. E.B., B.L., M.P. and F.Z. were supported by the STFC Consolidated Grant No. ST/X000648/1. B.L. was supported by the STFC Consolidated Grant No. ST/X00063X/1. B.L. and M.P. were supported by the STFC Consolidated Grant No. ST/T000813/1 and received funding from the ERC under the European Union's Horizon 2020 research and innovation program under

Grant Agreement No. 813942. D.M. was supported by a studentship awarded by the Data Intensive Centre for Doctoral Training, funded by the STFC grant ST/P006779/1. D.V. was supported by the STFC Consolidated Grant No. ST/X000680/1. F.Z. was supported by the Advanced ERC grant ERC-2023-ADG-Project EFT-XYZ.

High performance computing—This work used the DiRAC Data Intensive service (CSD3) at the University of Cambridge, the DiRAC Data Intensive service (DIaL3) at the University of Leicester and the DiRAC Extreme Scaling service (Tursa) at the University of Edinburgh, managed respectively by the University of Cambridge University Information Services, the University of Leicester Research Computing Service and by EPCC on behalf of the STFC DiRAC HPC Facility (www.dirac.ac.uk). The DiRAC service at Cambridge, Leicester, and Edinburgh are funded by BEIS, UKRI and STFC capital funding and STFC operations grants. DiRAC is part of the UKRI Digital Research Infrastructure. This work was supported by the Supercomputer Fugaku Start-up Utilization Program of RIKEN. This work used computational resources of the supercomputer Fugaku provided by RIKEN through the HPCI System Research Project (Project ID: hp230397). Numerical simulations have been performed on the Swansea SUNBIRD cluster (part of the Supercomputing Wales project). The Swansea SUNBIRD system is part funded by the European Regional Development Fund (ERDF) via Welsh Government.

Research Software Availability statement—The results presented in this contribution are expanded in Ref. [25]. The workflow used to analyse these data is available at Ref. [30]. The modified HiRep code with support for the LLR is available at [31]. It is based upon [26, 28].

Research Data Availability Statement—The raw data generated in support of this work, and processed data derived from it, are available in machine-readable format at Ref. [32]. See also Ref. [33], for a description of our approach to reproducibility and open science.

References

- [1] G. Panico and A. Wulzer, *The Composite Nambu-Goldstone Higgs*, vol. 913, Springer (2016), [10.1007/978-3-319-22617-0](https://doi.org/10.1007/978-3-319-22617-0), [[1506.01961](https://arxiv.org/abs/1506.01961)].
- [2] G. Cacciapaglia, C. Pica and F. Sannino, *Fundamental Composite Dynamics: A Review*, *Phys. Rept.* **877** (2020) 1 [[2002.04914](https://arxiv.org/abs/2002.04914)].
- [3] M. Cirelli, A. Strumia and J. Zupan, *Dark Matter*, [2406.01705](https://arxiv.org/abs/2406.01705).
- [4] E. Bennett, J. Holligan, D.K. Hong, H. Hsiao, J.-W. Lee, C.J.D. Lin et al., *$Sp(2N)$ Lattice Gauge Theories and Extensions of the Standard Model of Particle Physics*, *Universe* **9** (2023) 236 [[2304.01070](https://arxiv.org/abs/2304.01070)].
- [5] E. Witten, *Cosmic Separation of Phases*, *Phys. Rev. D* **30** (1984) 272.
- [6] ET collaboration, *Science Case for the Einstein Telescope*, *JCAP* **03** (2020) 050 [[1912.02622](https://arxiv.org/abs/1912.02622)].
- [7] C. Caprini et al., *Detecting gravitational waves from cosmological phase transitions with LISA: an update*, *JCAP* **03** (2020) 024 [[1910.13125](https://arxiv.org/abs/1910.13125)].

- [8] W.-C. Huang, M. Reichert, F. Sannino and Z.-W. Wang, *Testing the dark $SU(N)$ Yang-Mills theory confined landscape: From the lattice to gravitational waves*, *Phys. Rev. D* **104** (2021) 035005 [2012.11614].
- [9] J. Halverson, C. Long, A. Maiti, B. Nelson and G. Salinas, *Gravitational waves from dark Yang-Mills sectors*, *JHEP* **05** (2021) 154 [2012.04071].
- [10] Z. Kang, J. Zhu and S. Matsuzaki, *Dark confinement-deconfinement phase transition: a roadmap from Polyakov loop models to gravitational waves*, *JHEP* **09** (2021) 060 [2101.03795].
- [11] B. Lucini, M. Teper and U. Wenger, *The Deconfinement transition in $SU(N)$ gauge theories*, *Phys. Lett. B* **545** (2002) 197 [hep-lat/0206029].
- [12] S. Borsanyi, R. Kara, Z. Fodor, D.A. Godzieba, P. Parotto and D. Sexty, *Precision study of the continuum $SU(3)$ Yang-Mills theory: How to use parallel tempering to improve on supercritical slowing down for first order phase transitions*, *Phys. Rev. D* **105** (2022) 074513 [2202.05234].
- [13] T. Rindlisbacher, K. Rummukainen and A. Salami, *Confined-deconfined interface tension and latent heat in $SU(N)$ gauge theory*, *Phys. Rev. D* **112** (2025) 114507 [2506.15509].
- [14] M. Reichert, F. Sannino, Z.-W. Wang and C. Zhang, *Dark confinement and chiral phase transitions: gravitational waves vs matter representations*, *JHEP* **01** (2022) 003 [2109.11552].
- [15] R. Pasechnik, M. Reichert, F. Sannino and Z.-W. Wang, *Gravitational waves from composite dark sectors*, *JHEP* **02** (2024) 159 [2309.16755].
- [16] M. Panero, *Thermodynamics of the QCD plasma and the large- N limit*, *Phys. Rev. Lett.* **103** (2009) 232001 [0907.3719].
- [17] B. Lucini, A. Rago and E. Rinaldi, *$SU(N_c)$ gauge theories at deconfinement*, *Phys. Lett. B* **712** (2012) 279 [1202.6684].
- [18] K. Holland, M. Pepe and U.J. Wiese, *The Deconfinement phase transition of $Sp(2)$ and $Sp(3)$ Yang-Mills theories in $(2+1)$ -dimensions and $(3+1)$ -dimensions*, *Nucl. Phys. B* **694** (2004) 35 [hep-lat/0312022].
- [19] G. Cossu, M. D’Elia, A. Di Giacomo, B. Lucini and C. Pica, *$G(2)$ gauge theory at finite temperature*, *JHEP* **10** (2007) 100 [0709.0669].
- [20] M. Pepe and U.J. Wiese, *Exceptional Deconfinement in $G(2)$ Gauge Theory*, *Nucl. Phys. B* **768** (2007) 21 [hep-lat/0610076].
- [21] K. Langfeld, B. Lucini and A. Rago, *The density of states in gauge theories*, *Phys. Rev. Lett.* **109** (2012) 111601 [1204.3243].

- [22] K. Langfeld, B. Lucini, R. Pellegrini and A. Rago, *An efficient algorithm for numerical computations of continuous densities of states*, *Eur. Phys. J. C* **76** (2016) 306 [1509.08391].
- [23] B. Lucini, D. Mason, M. Piai, E. Rinaldi and D. VDACCHINO, *First-order phase transitions in Yang-Mills theories and the density of state method*, *Phys. Rev. D* **108** (2023) 074517 [2305.07463].
- [24] E. Bennett, B. Lucini, D. Mason, M. Piai, E. Rinaldi and D. VDACCHINO, *Density of states method for symplectic gauge theories at finite temperature*, *Phys. Rev. D* **111** (2025) 114511 [2409.19426].
- [25] E. Bennett, B. Lucini, D. Mason, M. Piai, E. Rinaldi, D. VDACCHINO et al., *Finite-temperature Yang-Mills theories with the density of states method: towards the continuum limit*, 2509.19009.
- [26] “GitHub - claudiopica/HiRep: HiRep repository — github.com.”
<https://github.com/claudiopica/HiRep>.
- [27] L. Del Debbio, A. Patella and C. Pica, *Higher representations on the lattice: Numerical simulations. $SU(2)$ with adjoint fermions*, *Phys. Rev. D* **81** (2010) 094503 [0805.2058].
- [28] “GitHub - sa2c/HiRep: HiRep repository — github.com.”
<https://github.com/sa2c/HiRep>.
- [29] D. Mason, B. Lucini, M. Piai, D. VDACCHINO and E. Rinaldi, *First-order phase transitions in Yang-Mills theories and the density of state method — HiRep LLR code v1.0.0*, July, 2023. 10.5281/zenodo.8134756.
- [30] E. Bennett, B. Lucini, D. Mason, M. Piai, E. Rinaldi, D. VDACCHINO et al., *Analysis release – finite-temperature yang-mills theories with the density of states method: towards the continuum limit*, 2025. 10.5281/zenodo.16579683.
- [31] D. Mason, E. Bennett, B. Lucini, M. Piai, D. VDACCHINO and E. Rinaldi, *The density of states method for symplectic gauge theories at finite temperature — HiRep LLR code v1.1.0*, Sept., 2024. 10.5281/zenodo.13807993.
- [32] E. Bennett, B. Lucini, D. Mason, M. Piai, E. Rinaldi, D. VDACCHINO et al., *Data release – finite-temperature yang-mills theories with the density of states method: towards the continuum limit*, 2025. 10.5281/zenodo.16580109.
- [33] E. Bennett, *The TELOS Collaboration Approach to Reproducibility and Open Science*, 2504.01876.